PULSED RESPONSE OF HIGH-SPEED SEMICONDUCTOR LASER (InGaAsP)

Anwar A. Aboul-Enein
Electrical Communication Department, Faculty of Electronic Engineering,
Menoufia University, Menouf-Egypt.

ABSTRACT

Digital response of high-speed semiconductor lasers has been modelled and investigated under different thermal conditions and no parasitic bonding pads. The widest digital modulation of InGaAsP diode lasers has been analyzed on the base of small amplitude model. Both the optical gain and the carrier concentration at transparency are correlated as temperature-dependent parameters of exponential forms. Three relevant items of major interest are studied to account for the thermal digital modulation of the optical device: i) the steady state response; its ultimate value, and the ratio between them ii) the 3-dB of the ratio above, and iii) the steady state harmonic response. The problem has been investigated under wide ranges of two major affecting parameters: the injected current and the device temperature.

1. INTRODUCTION

The field of high-speed semiconductor lasers has undergone substantial advances since the first demonstration of a laser with a modulation bandwidth beyond 10 GHz [1,2]. Such device are of great importance for optical communication systems due to the their small size, high efficiency, easy handling and controllability, and high speed for direct modulation which has been a subject of special emphasis and active research for the past 30 years.

There are three important factors to be considered to realize high-speed long-span transmission systems [3]: i) high frequency response of laser diodes, APD's and electrical circuits, ii) spectral characteristics of LD output, when directly modulated with high speed pulse streams, and iii) optical fiber dispersion and transmission loss characteristics.

Wide bandwidth transmission systems today utilize directly modulated In GaAsP laser with spectral linewidths of about 4nm, and In GaAs p-i-n or Ge-APD photodiodes [4].

By reducing active layer with of constricted-mesa lasers to 1μm, CW bandwidth has been increased to 16 GHz at 20°C and to 26.5 GHz at-60°C. The pulsed 20°C bandwidth was 22 GHz [5]. These mentioned data indicated that the present bandwidth limitation is predominantly thermal. A best-ever 22 GHz CW 3dB bandwidth was reported in Ref. [6] for a 1.3 μm InGaAsP vapour-phase-regrown buried heterostructure laser. The device was shown to have excellent modulation efficiency.

The differential gain of 1.3μm InGaAsP lasers was found to be a strong function of the active layer doping level [7]. A modulation bandwidth of 15 GHz was achieved, using devices with doping enhanced differential gain and short cavity lengths. To avoid the large wavelength chirping that accurse in a high-speed direct modulation, which severely limits the span-rate system product, the external modulation technique was employed [8], where a high frequency response ($\simeq$ 7 GHz) was measured with a small linewidth enhancement factor.

The modulation characteristics of InGaAsP laser diodes grown on p-type substrate have been studied experimentaly [9], on devices in which the parasitic bonding pads have been eliminated.

A small signal 3-dB bandwidth as high as 16.4 GHz has been measured. Also, the laser has responded to large-signal digital sequences at rates of 16 G bit/sec.

The dynamic behavior of 1.3 μm InGaAsP p-substrate buried crescent (PBC) lasers emitting maximum output powers of more than 30 m Watt//facet was characterized in detail [10] where a 3-dB modulation bandwidth of 11.5 GHz was observed.

To the best of our knowledge, no theoretical study for the thermal dependence of the physical parameters and its effect on the modulation bandwidth had been considered, thus in the present paper, and on the bases of the rate equations for a single-mode semiconductor laser

(InGaAsP) with uniform carrier distribution, the thermal dependent digital modulation bandwidth is modelled, analyzed, and investigated over wide range of the controlling parameters of such optical devices.

II. Basic Model and Thermal Analysis:

To examine the thermal-dependent digital modulation characteristics, consider the rate equations for single-mode semiconductor laser with uniform carrier distributions [11].

$$\frac{dN}{dt}=\frac{I}{qV}-g'(N-N_t)S-\frac{N}{\tau_n} \tag{1}$$

$$\frac{dS}{dt}=g'(N-N_t)\,S-\frac{S}{\tau_p}+\frac{B\Gamma N}{\tau_n} \tag{2}$$

where N and S are the electron and photon densities in the active layer, m^{-3}, I is the device current, q is the electron charge, V is the active layer volume, g′ is the differential gain, N_t, is the electron concentration at transparency, τ_n and τ_p are electron and photon lifetimes, B is the fraction of spontaneous emission coupled into the lacing mode, and Γ is the mode confinement factor. Based on microwave and mellimeter wave measurements the expression for gain saturation in a two-level system is taken as in [12].

$$g'=g_o/(1+\epsilon\, S) \tag{3}$$

Where ϵ is small parameter and $\epsilon S << 1$.
For small-signal

$$S = S_o + se^{j\omega t}$$

$$N = N_o + ne^{j\omega t}$$

$$I = I_o + ie^{j\omega t}$$

The frequency response of a laser without parasitic [11] is

$$G(j\omega) = \frac{1}{i} = \frac{A}{\omega^2 + jB\omega + C} \tag{4}$$

where A, B, and G are real

$$A = \frac{-1}{qV}\left(\frac{\Gamma g_o S_o}{1+\epsilon S_o}+\frac{\Gamma B}{\tau_n}\right)$$

$$B = \frac{-g_o S_o}{1+\epsilon S_o}-\frac{1}{\tau_n}\frac{\Gamma g_o(N_o-N_T)}{1+\epsilon S_o}-\frac{1}{\tau_p}$$

$$C=\left(\frac{g_o S_o}{1+\epsilon S_o}+\frac{1}{\tau_n}\right)\left(\frac{\Gamma g_o(N_o-N_T)}{1+\epsilon S_o}-\frac{1}{\tau_p}\right) - \frac{g_o(N_o-N_T)}{1+\epsilon S_o}\left(\frac{\Gamma g_o S_o}{1+\epsilon S_o}+\frac{\Gamma B}{\tau_n}\right)$$

The pulse transfer function G (z) for discrete analysis obtained as follows steps.

a- derivation of the corresponding transfer function usi Laplace transform G (s).
b- finding the weighting function g (t)
c- finding the z-transform of the weighting function (z).

Thus, the pulse transfer function G (z) is derived f Eq. (4) employing the above mentioned procedure as:

$$G(s) = \frac{S(s)}{I(s)} = -\frac{A}{s^2 Bs - C}$$

then

$$g(t) = A_o \exp\left(\frac{B}{2}t\right) \sin \omega_o t$$

where

$$\omega_o = \sqrt{(B^2/4)-C}$$

$$A_o = -A/\omega_o$$

and finally

$$G(z) = \frac{S(z)}{I(z)} = A_o\frac{zD}{z^2 - zE + F}$$

where

$$D = e^{BT_s/2}\sin\omega_o T_s$$

$$E = 2\cos\omega_o\ Te^{BT_s/2}$$

$$F = e^{BT_s}, \text{ and}$$

T_s is the sampling interval

It is known [13] that the sampled input signal applied to the continuous plant in a sampled data system can be treated as consisting of a series of impulses approximating the finite duration pulses which arise in the actual sampling process. The weigh of each impulse is equal to T_s y (kT_s) where y (kT_s) is the value of the input signal at sampling time $t = kT_s$. Using the inpulse approximation of the sample input signal, it can be shown that the unit step z-transform is given by

$$I(z) = \frac{T_s z}{z-1} \tag{8}$$

The use of Eq. (8) into Eq. (7) yields

$$S(z) = \frac{T_s z}{z-1}.G(z) \tag{9}$$

Taking the inverse z-transform, the discrete output signal

$$S(kT_s) = R_1 + R_2 + R_3 \tag{10}$$

where

$$R_1 = \lim_{z\to 1}(z-1)S(z)z^{k-1} = A_o T_s D.\frac{1}{1-E+F}, \tag{11}$$

$$R_2 = \lim_{z\to 1}(z-1)S(z)z^{k-1} = A_o T_s D.\frac{z_1^{k-1}}{(z_1-1)(z_1-z_2)}, \text{ and} \tag{12}$$

$$R_3 = \lim_{z\to 2}(z-z_2)S(z)z^{k-1} = A_o T_s D.\frac{z_2^{k-1}}{(z_2-1)(z_2-z_1)} \tag{13}$$

where

$z_{1,2} = \frac{1}{2}(E \pm \sqrt{E^2-4F})$ are the roots of: $z^2 + Fz + F = 0.0$

Starting from Eq. (7), the steady state response of a discrete time system [14] is

$$H(e^{j\omega t}) = A_o D T_s \frac{e^{j\omega t}}{e^{2j\omega t} - Ee^{j\omega t} + F} \tag{14}$$

The amplitude response of this function is derived as:

$$A(\omega t) = \sqrt{H(e^{j\omega t}H(e^{-j\omega t})}$$

$$= A_o T_s D[\sqrt{1+E^2+F^2-2E(1+F)\cos\omega t} + \sqrt{2F\cos 2\omega t}\ ]^{-1} \tag{15}$$

The normalized amplitude response $A_n(\omega t)$ is given as

$$A_n = A(\omega t)/A(o)$$

$$= \frac{1-E+F}{\sqrt{1+E^2+F^2 2E(1+F)\cos\omega t + 2\cos 2\omega t}} \tag{16}$$

Assuming that the overshoot, M, is required to be at $\omega_M T_s < \tau$, and taking into account that the cut-off occurs at $\omega_c T_s = \omega$ [13,14], we design the following criterion to calculate the maximum bandwidth at the overshoot i.e., $\omega_M = \omega_c$

$$\text{i.e.} \qquad \cos\omega_M T_s = -1$$

or

$$E(1+F) + 4F = 0.0$$

$$E + F(4+E) = 0.0 \tag{17}$$

Equation (17) yields the smallest sampling interval. The approximate solution of Eq. (17) gives

$$BT_{min} \simeq -1.5 \tag{18}$$

Thus, the highest sampling frequency is given as

$$f_{max} = \frac{1}{T_{min}} \simeq -\frac{1}{3}B \qquad (19)$$

Another approach to study the effect of the sampling interval is the steady state step response which is given as

$$S(\infty) = \lim_{z\to 1} \frac{z-1}{z} S(z) \qquad (20)$$

The use of Eq. (7) and Eq. (9) into Eq. (20) gives

$$S_{T_s}(\infty) = \lim_{z\to 1} A_o T_s D \frac{z}{z^2 - Ez + F}$$

$$= A_o T_s D. \frac{1}{1-E+F} \qquad (21)$$

$S(\infty)$ possesses an ultimate value, $S_u(\infty)$, when T approaches a zero value where

$$S_u(\infty) = \lim_{T_s\to 0} S(\infty) = -\frac{A}{(B^2/2)-C} \qquad (22)$$

which has a mathematical meaning only. A quantity of special interest is the ratio:

$$R(T_s) = \frac{S_{T_s}(\infty)}{S_u(\infty)} = \frac{(B^2/2)-C}{\sqrt{B^2/4)-C}} T_s D \frac{1}{1-E+F} \qquad (23)$$

A physical quantity of important interest is the sampling interval, T_{3dB}, corresponding to 3-dB point of $R(T_s)$ i.e. T_{3dB} is the solution of

$$10 \log R_o . \frac{T_s D}{1-E+E} = -3$$

or

$$R_o \frac{TD}{1-E+F} = \frac{1}{2} \qquad (24)$$

where

$$R_o = \frac{(B^2/2)-C}{\sqrt{(B^2/4)-C}}$$

RESULTS AND DISCUSSION

The advances in high speed semiconductor laser technology described in recent articles [1-12] have open up new areas of applications involving high-data-ra high speed analog and microwave transmission throu optical fibers.

In general, the three fundamental parameters t govern the modulation bandwidth of injection laser are the photon density, the injected current, and t optical gain.

Both the optical gain g_o and the threshold electr density N_T are temperature-dependent relevant physi parameters. Based on the data published in Ref. [15] a on the same spirit of Refs [16-19], the follow temperature-dependent correlations have been derived f both g_o and N_T where:

$$g_o(T) = g_o(300) \exp[-4.5 (T-300)/300] \quad (2$$

and

$$N_T(T) = N_T(300) \exp[2.4 (T-300)/300] \quad (2$$

Taking Eqs. (25) and (26) into consideration in t present paper, three relevant topics are studied in deta namely:

i- Steady state step response $S_{T_s}(\infty)$ and its ultim values, $S_u(\infty)$.

ii- The ratio of $S_{T_s}(\infty)/S_u(\infty)$.

iii- The 3-dB point of the ratio above.

iv- The steady state harmonic response of the devic

The above items are considered for the device und digital modulation.

The frequency (bit-rate) at which the ratio $S_{T_s}(\infty)/S_u(\infty)$ reaches to 3-dB and denoted as f_{3dB} displayed in Figures (1) and (2) where it is clear that:

i- f_{3dB} possesses a monotonic variation

ii- as the device is cooled, f_{3dB} increases.

iii- as the injection current increases, f_{3dB} al increases.

A simple quadratic relation is tailored, using cur fitting technique, under the form

$$f_{3dB} = f_o + f_1 I + f_2 I^2, \text{ GHz} \quad (2$$

where f_o, f_1, and f_2 are expressed as

$$f_o = 24.197 - 0.054324 T - 8.8201\times10^{-5} T^2 \quad (2$$

$$f_1 = 1514.4 - 8.2318 T + 0.013446 T^2 \quad (2$$

$$f_2 = -4092.0 + 23.646 T - 0.041804 T^2 \quad (3$$

I is in amperes and T is in °K.

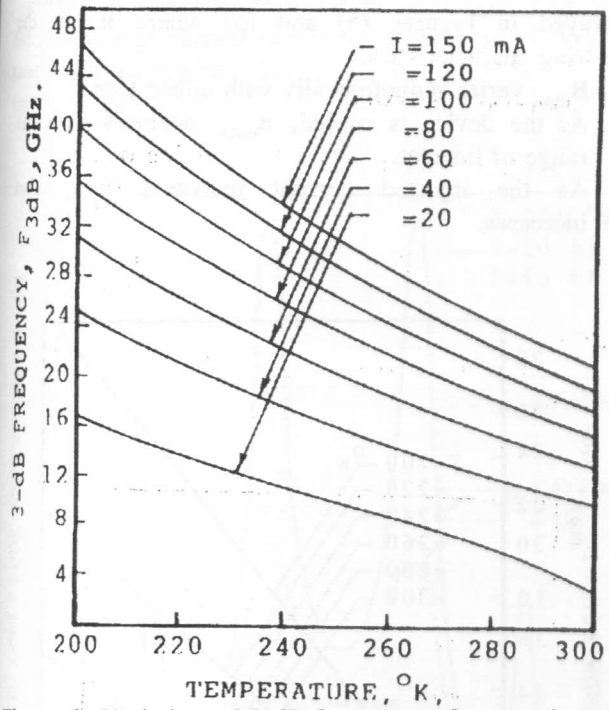

Figure 1. Variation of 3-dB frequency, f_{3dB}, against the variations of temperature, T, for different injected current, I.

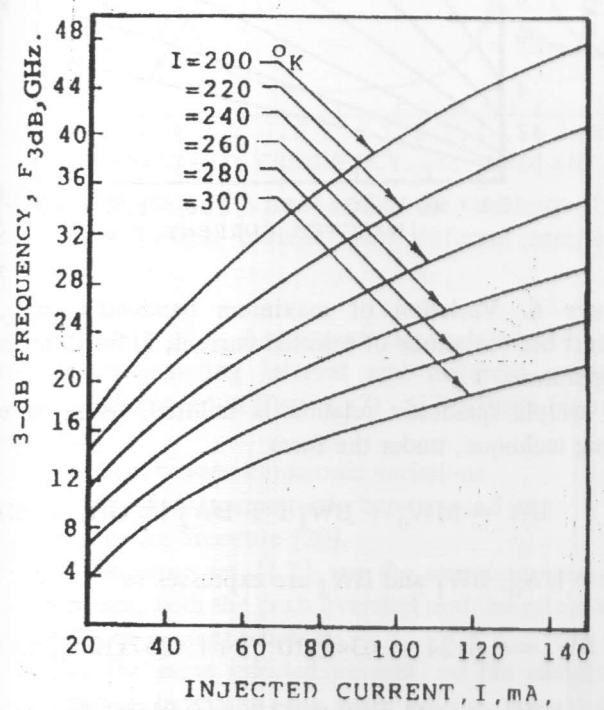

Figure 2. Variation of 3-dB frequency, f_{3dB}, against the variations of injected current, I, for different temperature, T.

The sampling interval corresponding to 3-dB bandwidth, T_{3dB}, is clarified in Figures (3) and (4) where T_{3dB} possesses the following characteristics:-

i- T_{3dB} possesses a monotonic variation,
ii- As the device is cooled, T_{3dB} decreases.
iii- As the injection current increases, T_{3dB} decreases.

A simple quadratic relation is tailored, using curve fitting technique, under the form

$$T_{3dB} = T_o + T_1 I + T_2 I^2, \text{ n sec.} \qquad (31)$$

where T_o, T_1, and T_2 are expresses as:

$$T_o = 1.3751 - 0.012194 T + 2.85517 \times 10^{-5} T^2 \qquad (32)$$

$$T_1 = -27.932 + 0.24809 T + 5.6547 \times 10^{-4} T^2$$

$$T_2 = 133.62 - 1.8677 T + 2.6896 \times 10^{-3} T^2 \qquad (33)$$

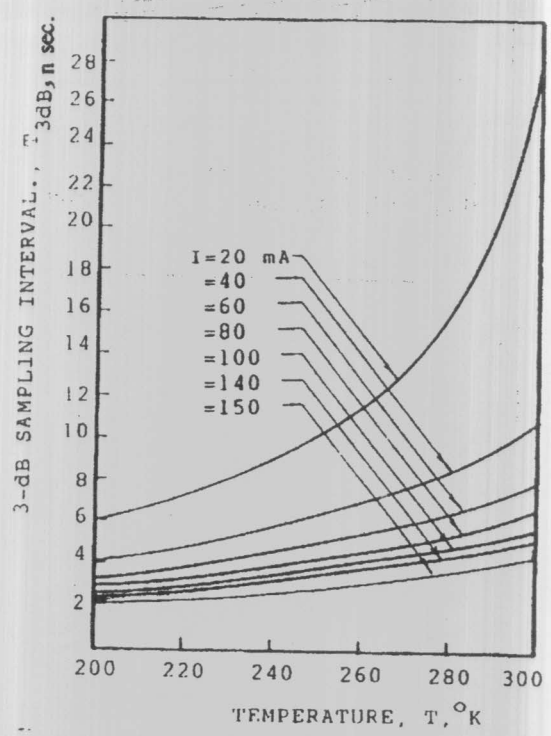

Figure 3. Variation of 3-dB sampling interval, T_{3dB}, against the variations of temperature, T, for different injected current, I.

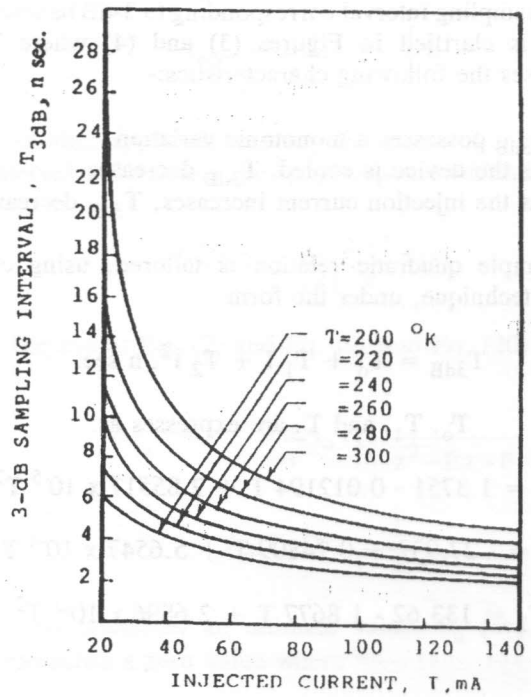

Figure 4. Variation of 3-dB sampling interval, T_{3dB}, against the variations of injected current, I, for different temperature, T.

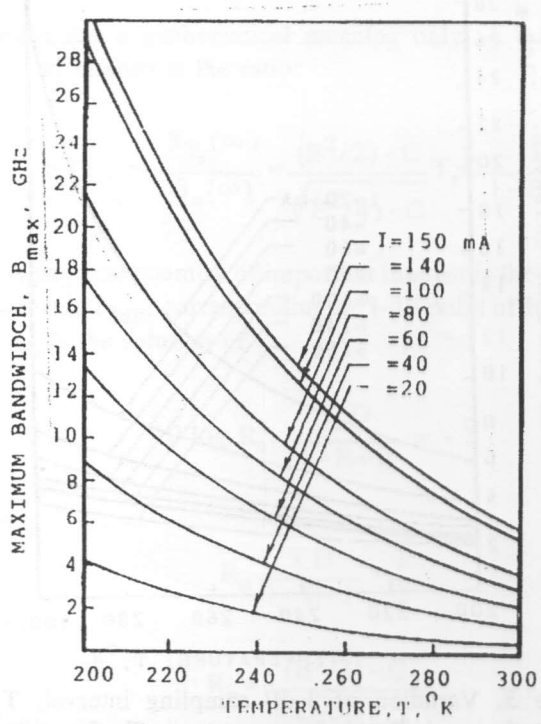

Figure 5. Variation of maximum bandwidth, B_{max}, against the variations of temperature, T, for different injected current, I.

The maximum bandwidth for digital processing B_{max} is portrayed in Figures (5) and (6) where it has the following characteristics:

i- B_{max} varies monotonically with either I or T

ii- As the device is cooled, B_{max} increases over the range of interest.

iii- As the injected current increases B_{max} also increases.

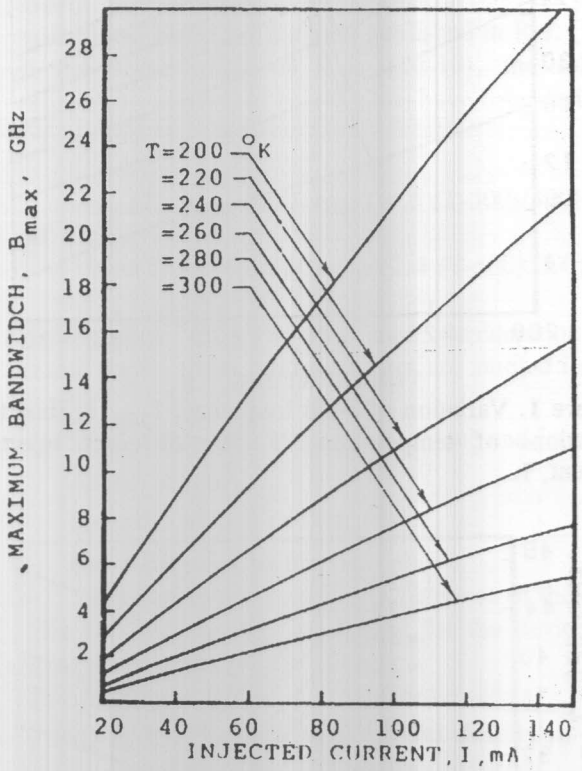

Figure 6. Variation of maximum bandwidth, B_{max}, against the variations of injected current, I, for different temperature, T.

A simple quadratic relation is tailored, using curve fitting technque, under the form

$$BW = MW_o + BW_1 I + BW_2 I^2, GH_z \quad (35)$$

where BW_o, BW_1 and BW_2 are expresses as

$$BW_o = -0.61241 - 3.6349 \times 10^{-3} T + 1.4257 \times 10^{-5} T^2 \quad (36)$$

$$BW_1 = 1607.4 - 9.9697 T + 0.01590 T^2 \quad (37)$$

$$BW_2 = -1907.4 + 11.248 T + 0.0187 T^2 \quad (38)$$

The above characteristics are in good agreement with the available published experimental work [6,9] over the range of interest where $200 \leq T\ (°k) \leq 300$ and $20 \leq I\ (mA) \leq 150$.

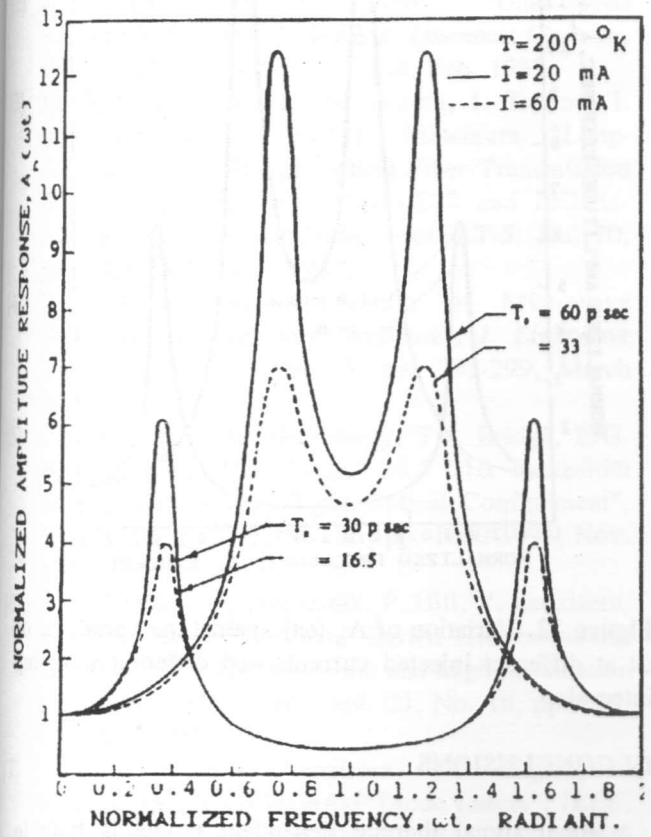

Figure 7. Variation of A_n (ωt) against the variations of ωt at different injected currents and different sampling intervals.

The variations of A_n (ωt) against the variations of ωt at different sampling interval and different injected current are displayed in Figures (7) - (12). These Figures clarify that

i- A_n (ωt) possesses monotonic variations

ii- A_n (ωt) has a symmetrical shape around $\omega t = \pi$ as given in the literature [20].

iii- For the same set {I,T}, as the sampling interval increases, both the peak overshot and the minimum values of A_n (ωt) increase.

iv- For the same injected current, as the sampling interval increases, the peak of the normalized amplitude response increases and shift to the higher normalized frequency.

v- As the injected current increase, the overall response shrinks but the maximum value and the minimum are at the same frequencies.

vi- For the same injected current, as the temperature increases, the 3-dB time interval T_{3dB} increases which in turns means the reduction of capacity of in for motion transmission. Such situation gives the tendency to cool the optical transmitter.

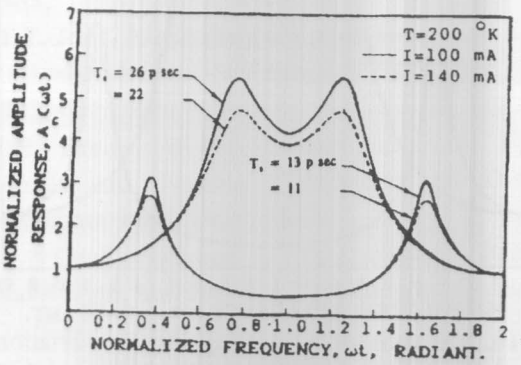

Figure 8. Variation of A_n (ωt) against the variations of ωt at different injected currents and different sampling intervals.

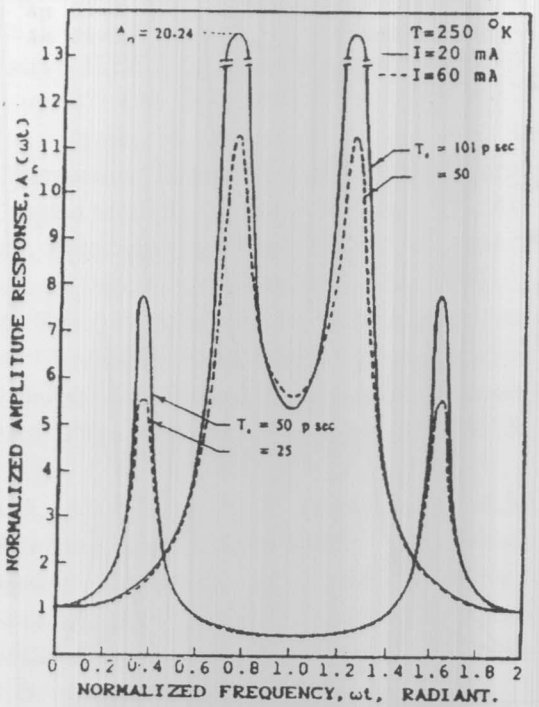

Figure 9. Variation of A_n (ωt) against the variations of ωt at different injected currents and different sampling intervals.

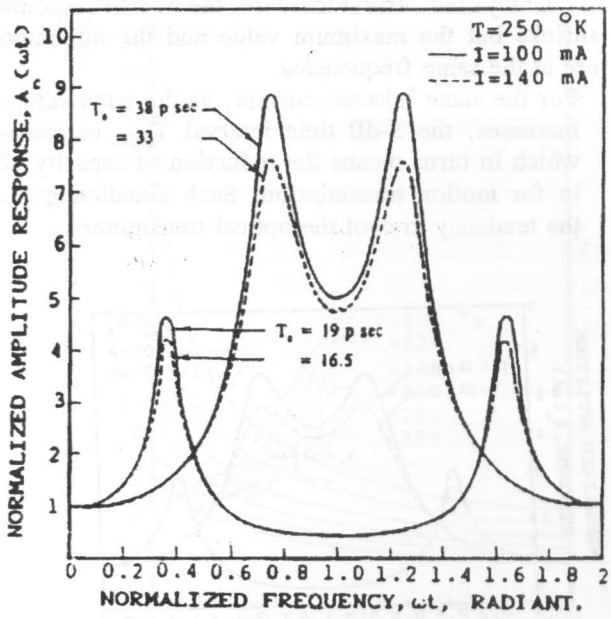

Figure 10. Variation of A_n (ωt) against the variations of ωt at different injected currents and different sampling intervals.

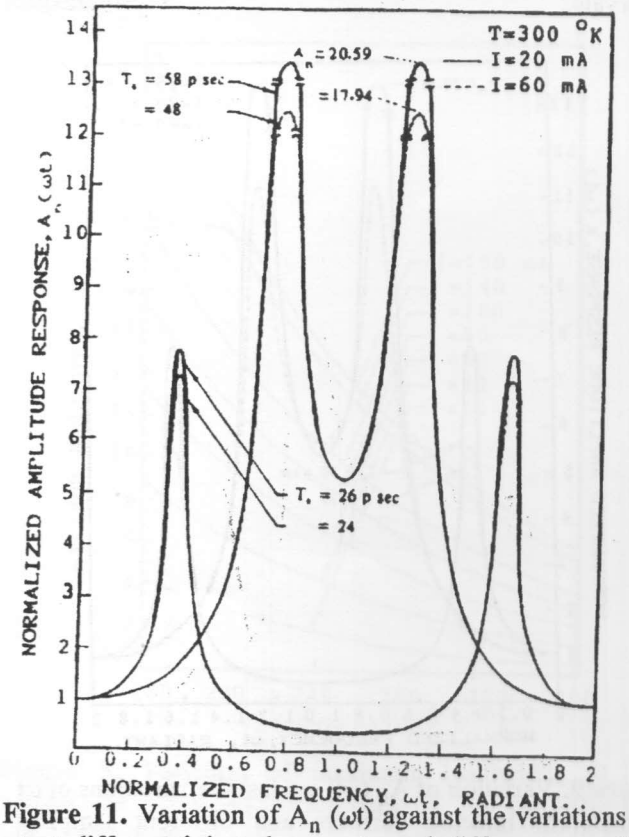

Figure 11. Variation of A_n (ωt) against the variations of ωt at different injected currents and different sampling intervals.

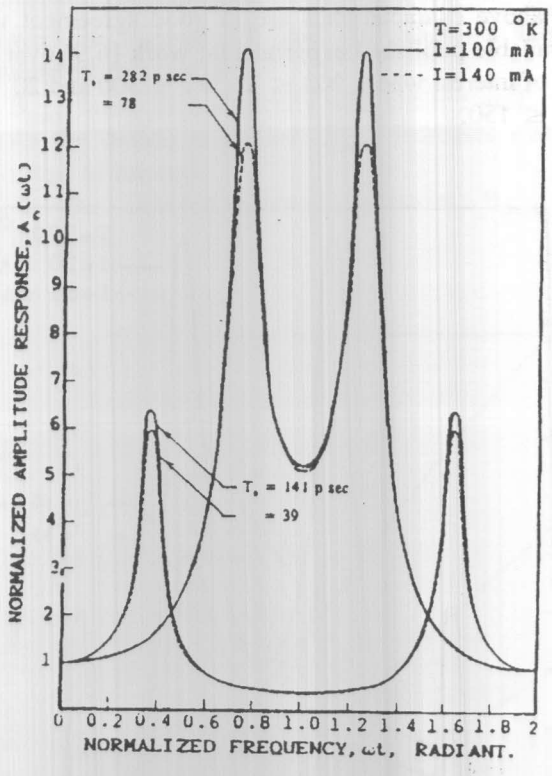

Figure 12. Variation of A_n (ωt) against the variations of ωt at different injected currents and different sampling intervals.

IV CONCLUSIONS

A small signal thermal dependent model is built to calculate the digital characteristics of InGaAsP laser device under the major affecting parameters, namely the active layer temperature an the injected current. Three relevant items of major interest are studied to account for the thermal digital modulation of the optical device i) The steady state step response and its ultimate value and the ratio between then ii) The 3-dB of the ratio above iii) The steady state harmonic response.

Under digital processing, the cooling of the optical device increases its bandwidth with a monotonic portrait cast under a simple quadratic form as function of the temperature, injected current and other physical and geometrical parameters. Also, as the injected current increases the device bandwidth increases which is in good agreement with the available published experimental work. The processed calculations clarify that the overall harmonic response increases the temperature increases and as the injected current decreases.

REFERENCES

[1] K.Y. Lau, "Short-Pulse and High Frequency Signal Generation in Semiconductor Lasers", *J. Lightwave Techn.*, vol. 7, No. 2, pp. 400-420, Feb. 1989.

[2] K.Y. Lau and A. Yariv., "Ultra-Speed Semiconductor lasers", *IEEE J. Quantum Electron*, vol. QE-21, No. 2, pp. 121-138, Feb. 1985.

[3] M. Shikada, S. Fujite, N. Henmi, I. Takano, I. Mito, K. Tasguchi, and K. Minemura, "Long-Distance Gigabit-Range Optical Fiber Transmission Experiments Employing DEB-LD'S and InGaAs-APD,s" *J. Lightwave Techn.*, vol. LT-5, No. 10, pp. 1488-1497, Oct., 1987.

[4] H. Sobol, "The Application of Microwave Techniques in Lightwave Systems", *J. Lightwave Techn.*, vol. LT-5, No. 3, pp. 293-299, March 1987.

[5] J.E. Bowers, B.R. Hemenway, T.J. Bridge, E.G. Burkhardt, and D.P. With," 26.5 GHz Bandwidth InGaAsP lasers with Tight Optical Confinement", *Elect. Lett.*, vol. 21, No. 23, pp. 1090-1091, Nov. 1985.

[6] R. Olshansky, W. Powazinik, P. Hill, V. Lanzisera, and R.B. Lauer, "InGaAsP Buried Heterostructure Laser with 22 GHz Bandwidth and High Modulation Efficiency", *Elect. Lett.*, vol. 23, No. 16, pp. 839-841, July 1987.

[7] C.B. Su and V.A. Lenzisera, "Ultra-High-speed Modulation 1.3 μm InGaAsP Diode Lasers", *IEEE, J. Quantum Elect.*, vol. QE-22, No. 9, pp. 1568-1577, Sep. 1986.

[8] M. Suzuki, H. Tanaka, S. Akiba and Kushiro, "Electrical and Optical Interaction Between Integrated InGaAsP/InP DEB Lasers and Electroabsorption Modulations", *J. Lightwave Techn.*, vol. 6, pp. 779-785, June 1988.

[9] D.Z. Tsong and Z.L. Liau, "Sinusoidal and Digital High Speed Modulation of p-Type Substrate Mass-Transported Diode lasers", *Lightwave Techn.*, vol LT-5, No.3, pp. 300-304, March 1987.

[10] W.W. Ng, R. Craig and H.W. Yen, "Dynamic Characteristics of High Speed p-Substrate InGaAsP Buried Crescent Lasers", *J. Lightwave Techn.*, vol. 7, No. 3, pp. 560-567, March 1989.

[11] J.E. Bowers, B.R. Hemenway, A.H. Gnauck and D.P. Wilt, "High-Speed InGaAsP Constricted-Mesa lasers" *IEEE J. Quantum Electron*, vol. QE-22, No. 6, pp. 833-844, June 1986.

[12] J.E. Bowers, "Millimeter wave response in InGaAsP lasers", *Electron Lett.*, vol. 21, pp. 1195-1197, 1985.

[13] M.T. Jong, Methods of Discrete Single and System Analysis, *McGraw-Hill Series in Elect. Eng.*, USA, 1982.

[14] R.E. Zimer, W.H. Tranter and D.R. Fannin, Signals and Systems Continuous and Discrete, *Macmillan Publ.* USA, 1983.

[15] H. Chafoori-Shiraz, "Temperature Bandgap-Wavelength, and Dopping Dependence of Reak-Gain Coefficient Parabolic Model Parameter for InGaAsP/InP Semiconductor laser Diodes", *J. Lightwave Techn.*, vol. 6, No. 4, pp. 500-515, April 1988.

[16] N.K. Dutta and R.T. Nelson, "Temperature Dependence of the lasing characteristics of the 1.3 μm InGaAsP/InP and GaAs-$Al_{0.35}$ $Ga_{0.46}$ As DH lasers", *IEEE J. Quantum Electron*, vol. Qe-18, No. 5, pp. 871-878, May 1982.

[17] E.A. Rezek, N. Holonyak, Jr and B.K. Fuller, "Temperature Dependence of Threshold Current for Coupled Multiple Quantum-Well In_{1-x} Ga_x As_z p_{1-z}- InP. Heterostructure laser Diodes", *J. Appl. Phys.*, vol. 51, No. 5, pp. 2402-2405, May 1980.

[18] M. Yano, H. Imai, and M. Takusagawa, "Analysis of Threshold Temperature Characteristics for InGaAsP/InP Double Heterojunction lasers", *J. Appl. Phys.*, vol. 52, No. 5, pp. 3172-3175, May 1981.

[19] A.A. Abou-Enein, F.Z. El-Halafawy, M.M. El-Halawany, and A.Abou-Koura, "Maximization of Analog Bandwidth of Optical Devices with Nonlinear Gain" *Modeling, simulation & Control, A, AMSE Press*, vol. 36, No. 2, pp. 23-33, 1991.

[20] S.D. Stearns and D.R. Hush, Digital Signal Analysis, *Prentic-Hall Int.*, 2nd Ed., U.S.A, 1990.